MTMW14 Project 2: Using Shallow Water Equations to Model Ocean Gyres

SN: 23865130

Introduction

In this project a model of a large scale ocean gyre is developed. The model is based on the Shallow Water Equations (SWEs), on a β-plane linearised about a resting state:

$$\frac{\partial \eta}{\partial t} = -H(\frac{\partial u}{\partial x} + \frac{\partial v}{\partial y}), \tag{1}$$

$$\frac{\partial u}{\partial t} = +(f_0 + \beta y)v - g\frac{\partial \eta}{\partial x} - \gamma u + \frac{\tau_x}{\rho H}, \tag{2}$$

$$\frac{\partial v}{\partial t} = -(f_0 + \beta y)u - g\frac{\partial \eta}{\partial y} - \gamma v + \frac{\tau_y}{\rho H}. \tag{3}$$

Here η represents the height perturbation, u and v represent the column averaged zonal and meridional velocity perturbations. H is the average height, f_0 and β are the Coriolis and β parameters, g is the acceleration due to gravity, γ represents drag processes, and τ_x and τ_y represent the wind stress forcings. The equations were solved using a square domain, with the sides being given by L. The values used for the parameters were:

parameter	value	unit
L	1×10^6	m
H	1000	m
f_0	1×10^{-4}	s^{-1}
β	1×10^{-11}	m^{-1} s^{-1}
g	10	m s^{-2}
γ	1×10^{-6}	s^{-1}
ρ	1000	kg m^{-3}
τ_x	$-cos(\frac{\pi y}{L})$	kg s^{-2}
τ_y	0	kg s^{-2}

Following Beckers and Deleersnijder (1993), the SWEs are solved on an Arakawa-C grid using the forward-backward time scheme. The Arakawa-C grid was chosen so that e.g. spatial derivatives of u in the x direction would be available at the points where η is calculated. The domain is taken to be the size of the η grid points, as can be seen in Fig. 1.

First η, u then v are calculated (in that order):

$$\eta^{n+1} = \eta^n - H\Delta t(\frac{\partial u^n}{\partial x} + \frac{\partial v^n}{\partial y}), \tag{4}$$

$$u^{n+1} = u^n + (f_0 + \beta y)\Delta t v^n - g\Delta t\frac{\partial \eta^{n+1}}{\partial x} - \gamma \Delta t u^n + \Delta t\frac{\tau_x}{\rho H}, \tag{5}$$

$$v^{n+1} = v^n - (f_0 + \beta y)\Delta t u^{n+1} - g\Delta t\frac{\partial \eta^{n+1}}{\partial y} - \gamma \Delta t v^n + \Delta t\frac{\tau_y}{\rho H}. \tag{6}$$

Second η, v then u are calculated (note, the order of u and v calculations has been swapped):

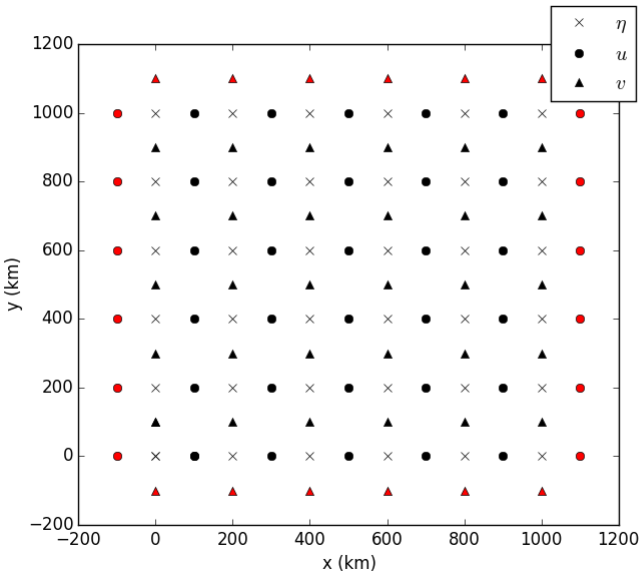

Figure 1: Shows where η, u and v are calculated on the Arakawa-C grid for $\Delta x = \Delta y = 200\,\text{km}$ (lower than the lowest resolution used in this project, for illustration only). Note, u is one bigger in the x direction than η (and similar for v in y direction), and therefore the minimum and maximum u coordinates lie $\frac{\Delta x}{2}$ outside the domain (and similar for v). The red grid-point values show values which are held at 0 due to the boundary conditions.

$$\eta^{n+2} = \eta^{n+1} - H\Delta t(\frac{\partial u^{n+1}}{\partial x} + \frac{\partial v^{n+1}}{\partial y}), \tag{7}$$

$$v^{n+2} = v^{n+1} - (f_0 + \beta y)\Delta t u^{n+1} - g\Delta t\frac{\partial \eta^{n+2}}{\partial y} - \gamma\Delta t v^{n+1} + \Delta t\frac{\tau_y}{\rho H}, \tag{8}$$

$$u^{n+2} = u^{n+1} + (f_0 + \beta y)\Delta t v^{n+2} - g\Delta t\frac{\partial \eta^{n+1}}{\partial x} - \gamma\Delta t u^{n+1} + \Delta t\frac{\tau_x}{\rho H}. \tag{9}$$

To calculate u on the other two grids (see Fig. 1), spatial averaging must be used. E.g. to calculate u on the η grid, the average of two u grid-points in the x direction must be used, and to calculate u on the v grid, four grid-points in the x and y directions must be used. Similar calculations apply to v and η on the other grids. Derivatives are calculated using the two values on either side of the grid-point where they are needed (using the midpoint method which is 2^{nd} order accurate, indeed this is the strength of the Arakawa-C grid).

Task A

To model the Western Boundary Current (WBC), a sufficient number of grid-points must span this distance. If the size of the WBC is taken to be $\frac{1}{10}$ $^{\text{th}}$ of the zonal extent of the domain, or 100 km, and four grid-points are required across this to capture its variation, this would mean a minimum spatial resolution of $\Delta x = 25\,km$ should be used. In this Task, a value of $\Delta x = \Delta y = 20\,km$ was used. Kinematic boundary conditions are used throughout this study, i.e. u is held at 0 on the eastern and western boundaries, v is held at 0 on the northern and southern boundaries (see Fig. 1).

The fastest signals propagating in this system are gravity-inertia waves. These have a phase speed of $\sqrt{gH}$, and following Beckers and Deleersnijder (1993), this can be used to calculate an upper bound for the CFL criterion, i.e.:

$$\sqrt{(\sqrt{gH}\frac{\Delta t}{\Delta x})^2 + (\sqrt{gH}\frac{\Delta t}{\Delta y})^2} <= \frac{1}{\sqrt{2}}, \tag{10}$$

will be a necessary condition for the scheme to be stable. In practice, at the first resolution, it was found that the less stringent requirement of

$$\sqrt{(\sqrt{gH}\frac{\Delta t}{\Delta x})^2 + (\sqrt{gH}\frac{\Delta t}{\Delta y})^2} <= 1 \tag{11}$$

was necessary to ensure numerical stability (from empirical experimentation). The first CFL criterion will be referred to as the strict criterion, and the second the lax criterion. In light of this, in this task Δt was taken to be 139 s so as to just satisfy this lax criterion. Satisfying the lax criterion allows for a larger timestep and therefore less time is needed to run the simulations.

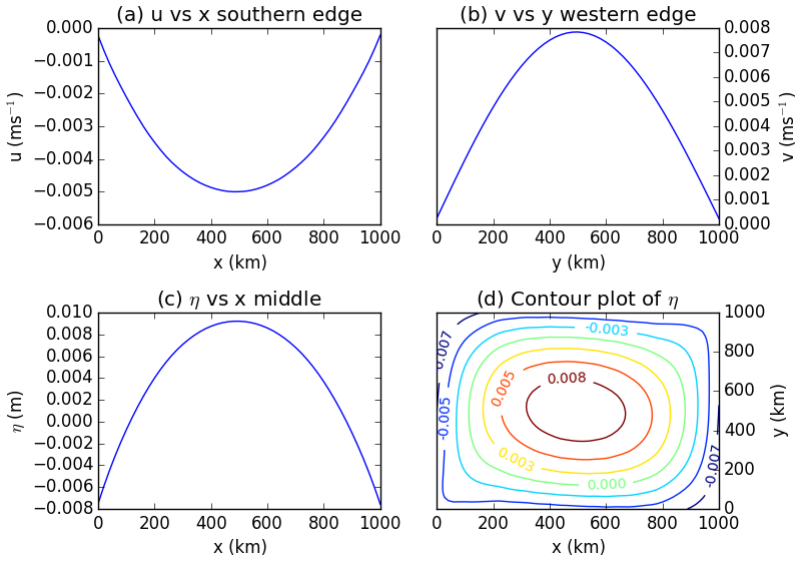

Figure 2: Four plots showing u, v and η along three different zonal/meridional extents after one day - (a), (b) and (c). Plot (d) shows η over the whole domain after one day.

The model was run for one day, and various plots of u, v and η are shown in Fig. 2. Overall, an anti-clockwise gyre is set up, as can be seen in plots (a) and (b) because u is negative along the southern boundary, and v is positive along the western boundary. Plot (d) shows that the height perturbation, η, is almost symmetrical after one day, although anomalously low values can be seen in the northeast and southwest corners.

Task B

The energy stored in the gyre can be calculated by summing the contributions from the kinetic energy (terms one and two in the integrand in Equation 12) and the gravitational potential energy (term three):

$$E(u, v, \eta) = \int_0^L \int_0^L \frac{1}{2}\rho(H(u^2 + v^2) + g\eta^2)dxdy \tag{12}$$

This can be approximated over the domain using Simpson's rule in 2D. This can then be calculated for every timestep, as is shown in Fig. 3. For this figure, the model was run at two resolutions: once as before with $\Delta x = \Delta y = 20$ km, and once with $\Delta x = \Delta y = 10$ km (i.e. twice the spatial resolution). A time step

of $\Delta t = 49$ s was use in both cases, so that the strict CFL criterion is just satisfied for the high resolution run and that only changes in the spatial resolution are being compared between the two runs. (It was found that running the model at the higher resolution with only the lax criterion being satisfied lead to numerical instability after around 100 days.) The model was run for 200 days in each case, and it can be seen that the energy reaches a peak at around 70 days before reducing by 2.05%(1.27%) for $\Delta x = 20$ km ($\Delta x = 10$ km) over the next 130 days. The variation from day 140 to day 200 is 0.0020% (-0.025%) for $\Delta x = 20$ km ($\Delta x = 10$ km), showing that the model has reached a steady state by day 200.

Task C

Given that the energy in the model has reached a steady state after 200 days, it can be compared to the steady state analytical solution as found in Musgrave (1985). The only unknown in these equations is the value of η_0, for which the modelled value of $\eta(0, \frac{L}{2})$ is used. One way of doing these comparisons is to work out the perturbations of u, v and η as defined by e.g. $u' = u - u_{st}$ (u_{st} is the steady state solution), then calculating the energy difference using Equation 12 - $E(u', v', \eta')$. Using this equation, when $\Delta x = 20$ km, the total energy difference between the analytical and the modelled steady state solution is 18.4 TJ, and when $\Delta x = 10$ km, the total energy difference is 4.99 TJ. Therefore, increasing the resolution increases the accuracy of the modelled steady state solution. The 2$^{\text{nd}}$ order spatial accuracy of the 2D SWE numerical model on an Arakawa-C grid can be seen from the fact that when the resolution is doubled, the error, as measured by the total energy difference, is approximately four times smaller.

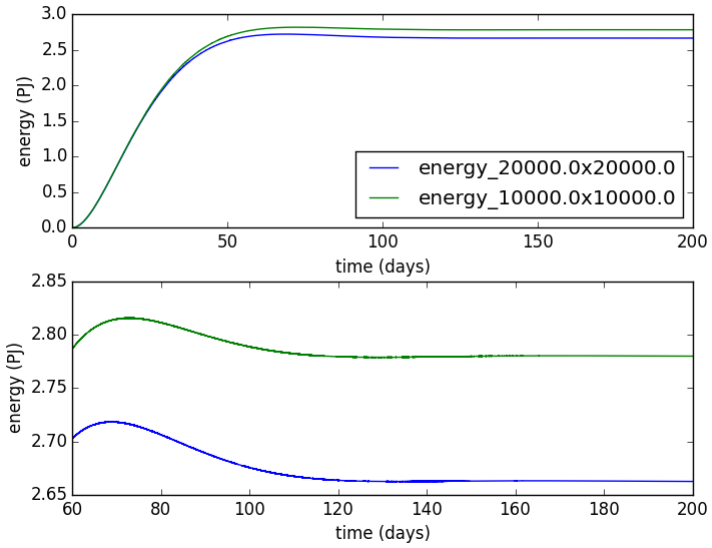

Figure 3: The effect of spatial resolution on the total energy of the system. Doubling the spatial resolution (blue curve) increases the overall energy of the system. It also reduces the energy difference between the analytical steady state solution and the steady state obtained by running the SWE model for 200 days.

Task D

One way of solving a non-linear version of the SWE equations is to implement a semi-Lagrangian numerical scheme. Here the full Lagrangian rates of change ($\frac{D}{Dt}$ as opposed to $\frac{\partial}{\partial t}$) are used, and the departure point of each of each grid-point is calculated to work out the previous value of u, v and η to be used. It is therefore necessary to calculate the departure points for each of the u, v and η grids used in the Arakawa-C grid. To calculate the departure point, the $\boldsymbol{u}$ = (u,v) field at two previous timesteps is used. Following Durran

pp366-368, first, a 2nd order estimate for $\boldsymbol{u}^{n+\frac{1}{2}}$ is calculated using $\boldsymbol{u}^{n+\frac{1}{2}} = \frac{3}{2}\boldsymbol{u}^{n} - \frac{1}{2}\boldsymbol{u}^{n-1}$. This is then used to calculate a value of $\tilde{\boldsymbol{x}}$, the departure point, through the use of an intermediate departure point using the following formulae:

$$\boldsymbol{x}_{*} = \boldsymbol{x}^{n+1} - \boldsymbol{u}(\boldsymbol{x}^{n+1}, t^{n})\frac{\Delta t}{2}, \tag{13}$$

$$\tilde{\boldsymbol{x}}^{n} = \boldsymbol{x}^{n+1} - \boldsymbol{u}(\boldsymbol{x}_{*}, t^{n+\frac{1}{2}})\Delta t. \tag{14}$$

$$\tag{15}$$

The departure points tell us where to take the values of u, v and η from the previous timestep. However, it is unlikely that these departure points will lie on grid-points, therefore it is necessary to interpolate between the values of these three fields to calculate the values at the departure points. This is achieved using the `RectBivariateSpline` class from the `scipy.interpolate` namespace. By default this uses a 2D cubic spline interpolation, and this was used to implement the interpolation of the three fields in this Task. It also gracefully handles the extrapolation of points which are outside of its domain by using the value of the nearest point in the domain of interpolation, which is useful for this study. Once the values of the u, v and η fields have been calculated at the departure points for the three grids, the same forward-backward time scheme used before is used to update the three fields.

Interestingly, the semi-Lagrangian scheme was found to be more unstable for larger values of Δt than the Eulerian scheme empirically. That it should be unstable is to be expected: inertia-gravity waves will still provide a limit on its stability. (Although this can be removed by treating inertia-gravity waves semi-implicitly - not done in this study) It was found that running at a 20 km resolution, a time resolution of 75 s was necessary for the semi-Lagrangian scheme to be stable. This is used below.

A comparison of the two schemes can be seen if Fig. 4, which shows plots of η for both schemes run with $\Delta x = \Delta y = 20\,\text{km}$, and $\Delta t = 75\,\text{s}$, after 1 day and 100 days. The two schemes are clearly very similar, with almost identical magnitudes for η after both time periods. However, the semi-Lagrangian scheme is less symmetrical after 100 days, which may be due to the fact that the equations that it is solving are the non-linear counterparts to the equations solved by the first scheme.

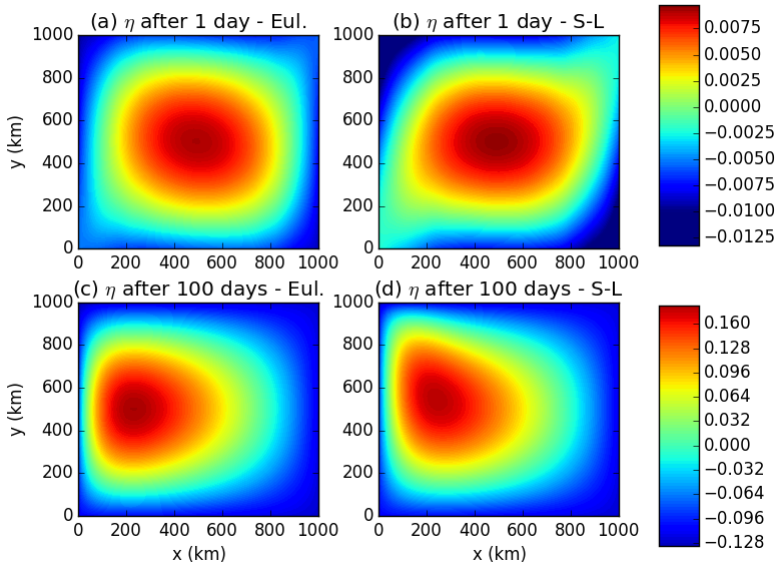

Figure 4: Contour plots of η for the original Eulerian scheme ((a) and (c)), and the semi-Lagrangian scheme ((b) and (d)) after 1 day and 100 days.

Finally, the total energy between the original Eulerian scheme and the semi-Lagrangian scheme can be compared, as is done in Fig. 5. Here, the two schemes are run again with the above settings for 100 days.

The two schemes give very similar energies throughout the run, with the semi-Lagrangian scheme having a consistently slightly higher energy, perhaps due to the asymmetries from the non-linearity as noted above.

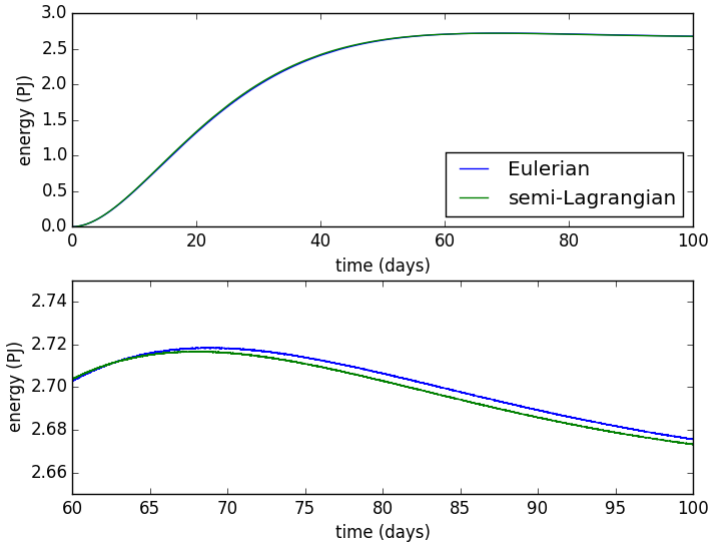

Figure 5: The total energy at each time for the original Eulerian scheme and the semi-Lagrangian scheme.

References

Beckers, J-M and E Deleersnijder (1993). "Stability of a FBTCS scheme applied to the propagation of shallow-water inertia-gravity waves on various space grids". In: *Journal of computational physics* 108.1, pp. 95–104.

Musgrave, D L (1985). "A numerical study of the roles of subgyre-scale mixing and the western boundary current on homogenization of a passive tracer". In: *Journal of Geophysical Research: Oceans* 90.C4, pp. 7037–7043.

Appendix A

All code can be downloaded from the following link:

https://github.com/markmuetz/mtmw14

All functions were coded using numpy array broadcasting instead of for loops, substantially speeding up the run time of the functions. The semi-Lagrangian scheme takes longer to run than the Eulerian scheme, due to the extra interpolation needed at each timestep.